A light–heat synergism in the sub-bandgap photocatalytic response of pristine TiO_2: a study of *in situ* diffusion reflectance and conductance

Zhizhou Wu,[a] Liuyang Li,[a] Xuedong Zhou,[a] Ivan P. Parkin,[b] Xiujian Zhao[a] and Baoshun Liu*[a]

Pristine TiO_2 materials are mainly used as photocatalysts under super-bandgap light illumination. The sub-bandgap (SBG) photocatalytic response has seldom been investigated and the mechanism of action remains unclear. In the current research, we firstly study the SBG light electronic transition of pristine P25 TiO_2 by means of *in situ* diffusion reflectance and (photo)conductance measurements under finely controllable conditions. It is revealed that the SBG light can promote valence band (VB) electrons to the exponentially-distributed gap states of the TiO_2, which can then be thermally activated to the CB states. A hole in the VB and an electron in the CB can be generated by the synergism of a SBG photon and heat. It is also seen that the photoinduced electrons can transfer to O_2 through the CB states, and that the holes can be captured by isopropanol molecules. As a result, isopropanol dehydrogenation can occur over pristine TiO_2 under SBG light illumination. It is seen that the photocatalytic activity increases with temperature and the energy of the SBG photons, in agreement with the light + heat synergistic electric transition *via* the exponential gap states. The present research reveals a mechanism for the SBG light photocatalytic response of pristine TiO_2 materials, which is important in designing highly-active visible light active photocatalysts.

1. Introduction

The replacement of fossil fuels with renewable energies is becoming more and more urgent under a desire to cut CO_2 emissions to limit the global temperature rise. Semiconductor photocatalysis is a meaningful strategy to address this problem by using solar energy and will still draw much attention in the future.[1–5] Super-bandgap (where the photon energy is larger than the bandgap) excitation is mainly considered for pristine semiconductors in photocatalytic studies.[6–8] Taking TiO_2 materials as examples, the super-bandgap light corresponds to UV light, which only accounts for ~4% of the total solar energy reaching the Earth's surface. TiO_2 has many advantages, including high stability, cheapness, and environmental-friendliness, so it is always unexpected for visible light to be efficiently used in photocatalysis. General ideas to improve the visible light activity include extra dopants into the lattice; this however might be harmful for the photocatalytic activity as the recombination of electron–hole pairs will be increased.[9,10] Moreover, artificial dopants can also lead to a decrease in the thermal stability and durability of TiO_2 materials.[11]

For undoped pristine TiO_2 materials, it has been found that they can respond to light with a photon energy lower than the band gap energy (E_g), *i.e.*, the sub-bandgap (SBG) light response, although the efficiency is much lower than that of the super-bandgap response. For example, it has been reported that photoelectrochemical (PEC) water oxidations can occur over pristine rutile TiO_2 anodes and $SrTiO_3$ under SBG light illuminations;[12,13] we recently saw that SBG light illumination can result in a relatively high PEC property over TiO_2 nanorod arrays.[14] The SBG light response might be dependent on the TiO_2 type. It was also seen in our previous study that pristine P25 TiO_2 virtually does not respond to SBG light in PEC water oxidation.[14]

As a SBG photon cannot promote a valence band (VB) electron to the conduction band (CB) of TiO_2, a single SBG

[a] *State Key Laboratory of Silicate Materials for Architectures, Wuhan University of Technology, Wuhan City, Hubei Province, China. E mail: bshliu@whut.edu.cn*
[b] *Department of Chemistry, Materials Chemistry Centre, University College London, London, WC1H 0AJ, UK*

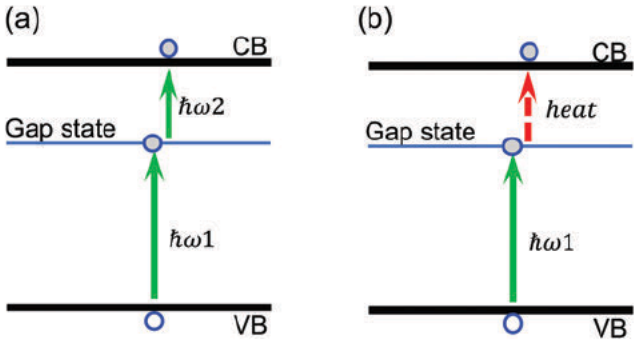

Fig. 1 (a) Diagram of the two SBG photon induced electronic transitions from the VB to the CB with a gap state being the relay level: (b) Diagram of the SBG photon heat synergistic electronic transition from the VB to the CB with a gap state being the relay level.

photon only cannot contribute to the photocurrent. It is thus considered in this research[12–14] that two SBG photons might couple to excite an electron from the VB to the CB with the gap states acting as the relay levels, as shown in Fig. 1a. In addition to this double photon mode, a VB electron excited to the gap states by a SBG photon may also be thermally activated to the CB state, as shown in Fig. 1b.[15] This mode includes a synergism of a SBG photon and heat. Whether such a synergism can cause a VB to CB electron transition in pristine TiO_2 and contribute to a photocatalytic effect is not well discussed in the literature.

We recently developed an *in situ* diffusion reflectance and a photoconductance measurement system that can work under finely-controllable conditions.[12,16,17] In the present research, by means of these methods, the SBG light response in commercial P25 is clearly observed, although the TiO_2 almost has no visible absorption in its diffusion spectrum. It is revealed that the exponentially-distributed gap states below the CB edge are involved in the SBG light–heat synergism for the electron transition from the VB of the pristine TiO_2 to its CB. The SBG light illumination causes isopropanol dehydrogenation that can contribute to the SBG light–heat synergistic electronic transition. The findings of the current research provide some new insights on the utilization of visible light in photocatalysis over pristine materials, not limited to TiO_2.

2. Experimental details

2.1. UV–Vis diffusion reflectance and cyclic voltammetry measurement

The UV–Vis diffusion absorption spectrum of the TiO_2 powder and the transmittance spectra of the optical filters were measured with a UV–Vis spectrophotometer (UV-2600, Shimadzu, Japan). To see the effect of isopropanol adsorption over the TiO_2 surfaces on the transmittance spectrum of TiO_2, a TiO_2 thin coating was coated over a quartz substrate (10 mm × 10 mm) through the doctor-blading of P25 TiO_2 paste (Heptachroma company, Dalian, China), and was subject to post-annealing at 450 °C for 1 h. The thickness of the TiO_2 was observed with an atomic force microscope (AFM, Nanoscope IV, VEECO, America) to be *ca.* 1.5 μm (Fig. S1, ESI†). A self-designed *in situ* optical cell,[18] which can be assembled into the UV–Vis spectrophotometer, was used to check the effect of isopropanol adsorption on the sample transmittance at room temperature in pure N_2 and isopropanol standard gas (500 ppm isopropanol in N_2). For the cyclic voltammetry (CV), a TiO_2 thin coating was coated on a FTO glass substrate (30 mm × 10 mm) according to the above method. The CV was obtained in an air-tight glass electrochemical cell containing 0.1 M Na_2SO_4 solution by an electrochemical station (CHI-760E, Shanghai Chenghua, China) in the dark at a scanning rate of 0.02 V s^{-1} at room temperature. The TiO_2 coating, a saturated calomel electrode, and a piece of Pt foil (10 mm × 10 mm) were used as the working, reference, and counter electrodes, respectively. The pH value was adjusted to ~2.5 with a diluted H_2SO_4 solution. Highly-purified N_2 was continuously bubbled throughout the whole CV measurement.

2.2. *In situ* diffusion absorption and vacuum photoconductance measurement

In-situ diffusion reflectance was measured with self-designed equipment (referring to our previous study[16]). *In situ* optical reflectance is a general method that can be used to monitor the electronic state change of a material under simultaneous light illumination. Taking TiO_2 as an example, light illumination could promote the VB holes to the CB or the gap states, which can then cause a broad absorption from the visible light region to the near IR light region. The absorption intensity is proportional to the electron concentration in TiO_2. Therefore, the dynamic change in the electron concentration can be monitored by an *in situ* diffusion reflectance at a wavelength under controllable conditions. In the current research, the changes in the diffusion reflectance at the 1550 nm laser were measured to reflect the change of the photoinduced electron concentrations under the excitations of 450 nm, 532 nm, and 630 nm lasers, in the presence of methanol and O_2 atmospheres. Anhydrous $BaSO_4$ was used as the reference, and the pristine P25 powder was used for measurement without further treatment. Highly-purified N_2 was firstly flowed through a glass bottle containing HPLC grade liquid isopropanol at a rate of 0.2 NL per min, and then through the sample cell. The diffusion reflectances of the 1550 nm laser were firstly measured in the dark, under laser illumination, and after the end of the laser excitation at different temperatures. Lastly, a highly-purified O_2 stream was flowed though the sample cell at 0.1 NL per min, and the diffusion reflectances were also measured. The diffusion absorptions of TiO_2 ($A(t)$) were calculated according to the following equation.

$$A(t) = 1 \quad \frac{R(t)}{R_{ref}} \qquad (1)$$

where $R(t)$ is the diffusion reflectance of TiO_2 at time t, and R_{ref} is the reflection of the anhydrous $BaSO_4$ reference.

Photoconductances were conducted in a self-designed platform under vacuum conditions.[10,17] A 50 μm wide strip of the FTO coating in the middle of a 20 mm × 10 mm FTO glass was removed by laser etching. A TiO_2 coating was then coated on

this strip through doctor-blading of the P25 TiO_2 paste, which was subject to a post-annealing at 450 °C for 1 h. The conductances were obtained with a Keithley-2450 source meter in the four-probe mode at different temperatures under a 2 V bias voltage. The sample chamber was firstly evacuated until the base pressure was *ca.* 3×10^{-2} Pa, and the pure N_2 or pure O_2 was introduced to obtain a 10 Pa partial pressure. 450 nm and 632 nm lasers were used as the excitation light sources. Light intensities were checked with the Newport Si-based photodetector (818-UV/DB, Newport, America). Thermally stimulated currents (TSC) were measured according to the following procedure under vacuum conditions at a bias voltage of 10 V. Firstly, the TiO_2 coating was illuminated with the 450 nm laser for 20 min at room temperature, which was then followed with a sharp decrease to −173 °C at a rate of 40 °C min^{-1}. The illumination was kept at −173 °C for 5 min, and then was switched off. At the moment of light interruption, the temperature was increased to 150 °C at 30 °C min^{-1} with a simultaneous measurement of the current, which was also measured according to the same procedure for the TiO_2 sample without light illumination.

2.3. Photocatalytic activity measurement

The commercial P25 powder was used without further modification. 0.1 g of the pristine p25 powder was mixed with deionized water to form a uniform slurry; this was coated on a ϕ 60 mm quartz substrate, and then dried at 70 °C in air. Catalytic experiments were performed in a self-designed quartz reactor (Fig. S2, ESI†) placed upon a heating plate. The surface temperatures of the sample was checked with a K-type thermocouple. A 500 W Xenon lamp, together with different optical filters that allow the transmission of light with specific wavelengths, was used as the light source to illuminate the sample downwards through a condenser. The light intensities were determined by a Newport Si-based photodetector (818-UV/DB). Isopropanol was used for catalytic dehydrogenation. The ratio of ∼500 ppm isopropanol-containing N_2 standard gases and pure O_2 was controlled with two mass flow meters to be 5 : 1 to flow through the reactor for ∼30 min to obtain a steady isopropanol concentration. After that, the reactor was connected to a gas chromatograph (GC-SMART, Shimadzu, Japan) with plastic tubes to form a closed reaction system. The evolution of acetone was checked in the dark and under light illumination. The by-products were determined by mass spectroscopy (GC-MS: Agilent 6890N/5975). The light induced surface temperature rise was confirmed with an infrared thermographic camera (FTIR-E60, America).

3. Results and discussions

3.1. SBG light response

As the pristine P25 does not exhibit an absorption below the CB edge in the diffusion absorption spectrum (Fig. S3, ESI†, dashed line), it is unexpected that the SBG light can cause an electronic transition. *In situ* diffusion reflectance was firstly used to check the SBG light response. If the SBG light illumination can excite an electronic transition in the pristine TiO_2, the photoinduced electrons, either in the CB or at the gap states, can result in a near infrared optical absorption.[19,20] Under 450 nm laser illumination, it is seen from Fig. 2a that the TiO_2 shows an absorption at 1550 nm in the absence of isopropanol; this is ascribed to the desorption of the chemisorbed O_2 over the TiO_2 surface under SBG light illumination.[21,22] The presence of isopropanol leads to a great increase in the optical absorption; this means that the SBG light illumination can extract electrons from isopropanol molecules to the TiO_2. It is also worth noting that the 0.05 value cannot be treated as the background absorption, but the apparent absorption of TiO_2 relative to the $BaSO_4$, so this does not mean that the P25 TiO_2 has a real absorption of 0.05 before light illumination. We therefore thought that this value should be meaningless. As a result, it is seen that the pristine TiO_2 can respond to the SBG light illumination. As the photon energy of the 450 nm laser is too low to induce the superbandgap electronic transitions, the interaction of isopropanol molecules with the TiO_2 surface is thought to cause the observed response. The effect of isopropanol adsorption on

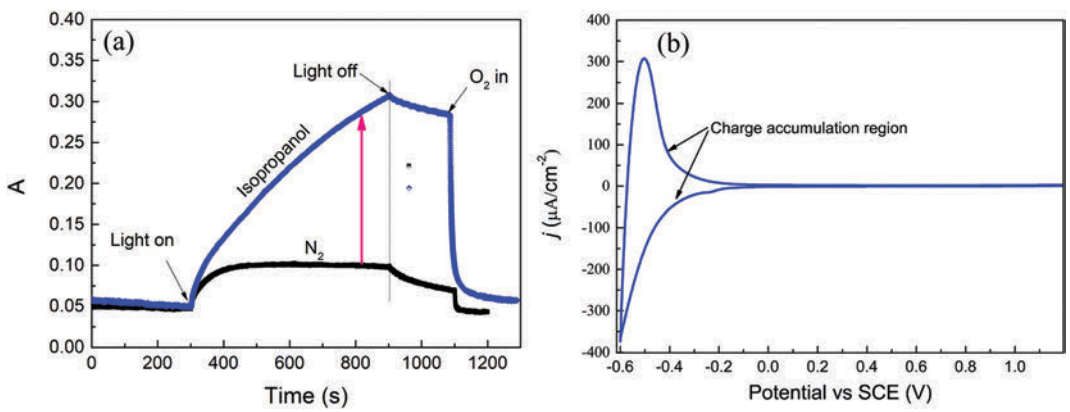

Fig. 2 (a) Evolution of the light induced absorptions at 1550 nm under and after the interruption of the 450 nm laser illumination in pure N_2 and the isopropanol containing N_2 at 40 °C (laser power: 400 mW); (b) cyclic voltammetry plot of the P25 coating obtained in a three electrode electrochemical cell containing 0.1 M Na_2SO_4 solution.

the transmittance spectra of the TiO_2 was checked (Fig. S4, ESI†); this, however, reveals no additional absorptions that are caused by the isopropanol–TiO_2 interaction, so the observed SBG light response should be ascribed to the TiO_2 material itself.

Thus, it is considered that the SBG light response should arise from an electric transition involving the gap states formed from some intrinsic defects and surface disorder in the nano-TiO_2.[23–25] As shown in Fig. 2b, the electrochemical cyclic voltammetry (CV) curve of the TiO_2 presents the capacitive features related to the charge filling/emptying of the gap states. It is also seen that the relaxations of photoinduced absorptions of the TiO_2 are dispersive due to the presence of the gap states under gaseous conditions,[26–28] and could be finely fitted if the gap states were involved in the kinetics model.[18,29] Other studies have also shown that the trapping effect of the gap states must be considered to understand the electron transport in nano-TiO_2.[30,31] Based on the CV and the results in the literature, it is considered that the gap states of the pristine TiO_2 should distribute below the CB edge as an exponential band tail. Such gap states are empty and allow an electronic transition from the VB to them under SBG light illumination. Fig. 3a shows the variation of the photoinduced absorptions at 1550 nm under 450 nm, 532 nm and 635 nm laser illuminations. It is seen that the absorption shows a nonlinear rapid increase as the light wavelength decreases from 635 nm to 450 nm; this agrees with the conclusion that the exponential gap states are involved in the SBG light response.

After the end of light illumination, the absorption shows a slight decrease; this is ascribed to the electron transfer from TiO_2 to the residual O_2 in the reaction chamber. The absorptions present a sharp decrease when gaseous O_2 is introduced, which shows that the SBG light induced electrons can transfer to O_2. The absorption at 1550 nm under 450 nm laser excitation was also measured at different temperatures, as shown in Fig. 3b. It is seen that the absorption relaxations increase with temperature, showing an increase in the electron transfer to residual O_2 with temperature (Fig. S5, ESI†). The kinetic constants just after the interruption of light illumination are obtained from the following equation.[32]

$$k_{et}(0) = \frac{1}{A(0)}\frac{dA(0)}{dt} \quad (2)$$

where $A(0)$ is the absorption at the moment the light is terminated. The E_{app} of the apparent activation energy of the electron transfer from the TiO_2 to the residual O_2 is estimated to be $\sim$13 kJ mol^{-1} (Fig. S5, ESI†).

3.2. Light–heat synergism in the SBG light response

The electrons localized at the gap states should be immobile because of their localized feature, and they must be activated to the CB states before transferring to O_2. To show this mechanism, photoconductances were also measured under 450 nm laser illumination, as shown in Fig. 4a. The high photoconductances shows that the SBG light illumination can indeed generate conductance electrons in the CB states. A great decrease in the photoconductance when gaseous O_2 was introduced means that the SBG light induced electrons can be transferred to O_2 *via* the CB states. Fig. 4b shows the effect of the temperature on the photoconductance in the presence of O_2. At the end of the light illumination, it is seen that the conductance relaxations, which are attributed to electron transfer to O_2,[33] increase with temperature;[34] this is also in good accordance with the *in situ* reflectance measurements.

The above results show that the SBG light induced electrons in gap-states can be activated to the CB. According to Fig. 1a, a trapped electron might be excited to the CB by another SBG photon. Thus, the photoconductances under 635 nm, 450 nm, and 450 nm + 635 nm laser illuminations are compared, as shown in Fig. 5a. It is seen that the 635 nm laser illumination leads to low photoconductance and has a minor effect on the 450 nm laser induced photoconductance. Therefore, the SBG induced photoconductances cannot be ascribed to the double-photon mode. It is considered that the electrons at the gap states should be activated to the CB by heat; this is supported by the photoconductances that increase with temperature from

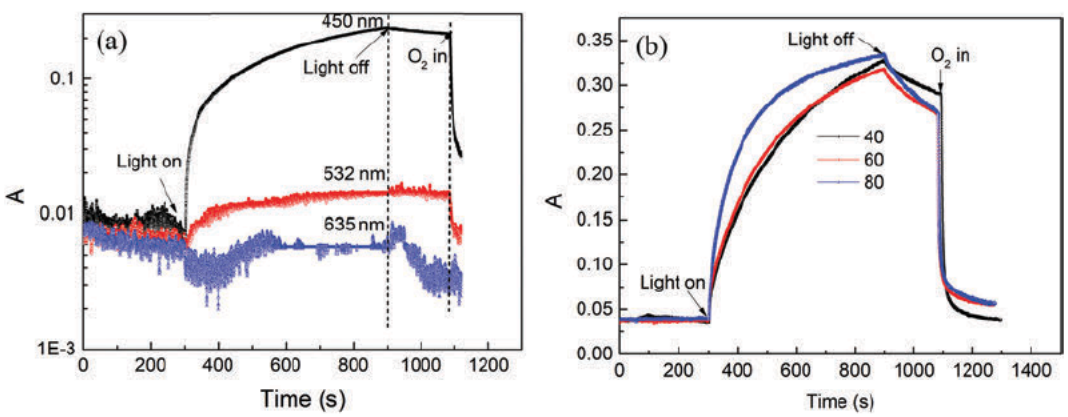

Fig. 3 (a) Evolution of the absorptions at 1550 nm under different laser illuminations in an isopropanol containing N_2 atmosphere at 40 °C (laser power: 400 mW for 450 nm, 210 mW for 532 nm laser and 400 mW for 635 nm laser); (b) evolution of the photoinduced absorptions at 1550 nm under 450 nm laser illumination at different temperatures (laser power: 400 mW).

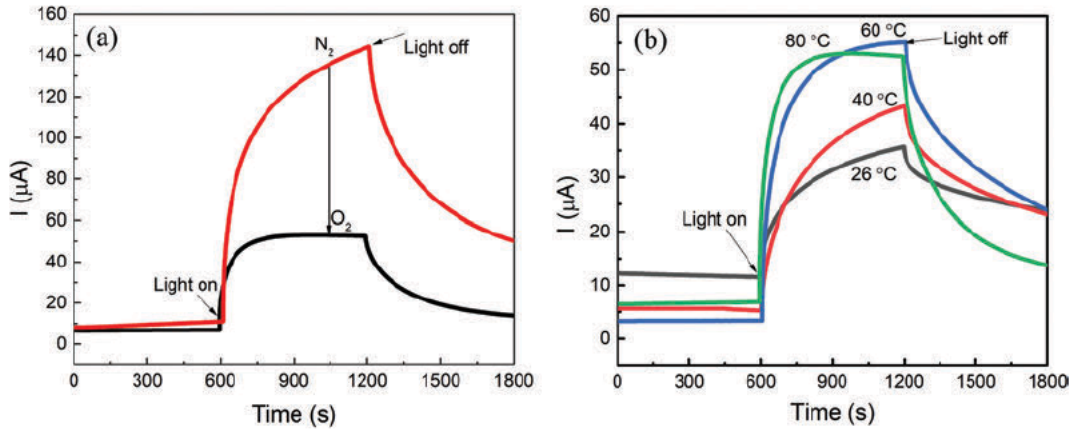

Fig. 4 (a) Evolution of the 450 nm laser induced photoconductance in 10 Pa N_2 and O_2 at 80 °C (laser power: 300 mW); (b) evolution of the 450 nm laser induced photoconductance at different temperatures in 10 Pa O_2 (laser power: 300 mW).

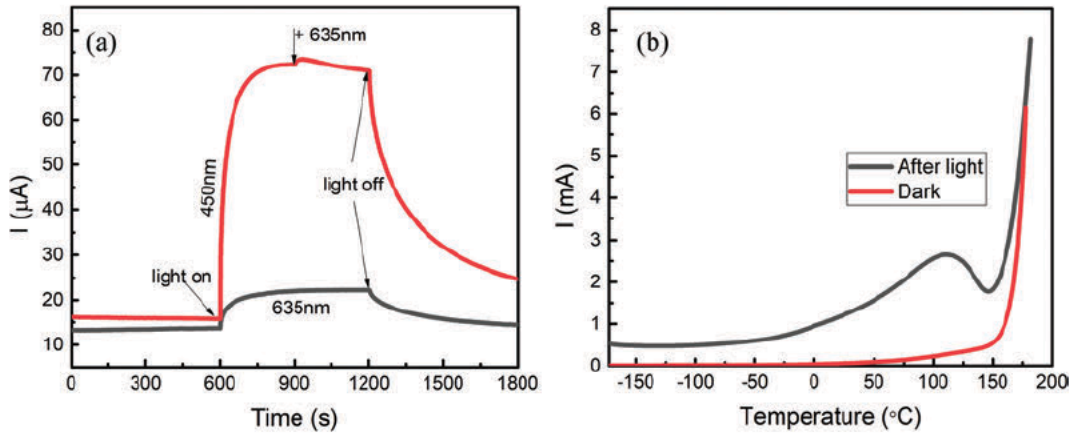

Fig. 5 (a) Evolution of the photoconductance under 450 nm (300 mW), 635 nm (300 mW), and 450 nm + 635 nm laser illumination in the presence of 10 Pa O_2 at 80 C; (b) TSC measurement when the film had been (black) and had not been (red) subjected to 20 min of 450 nm laser illumination at room temperature.

26 to 60 °C (Fig. 4b). The slight decrease in photoconductance at 80 °C is attributed to the increase of electron transfer to O_2. Thermally stimulated currents (TSC) were also used to confirm the thermal activation of the SBG light induced electrons to the CB states, which has been shown to be a useful way of detecting and analyzing sub-band level mediated electron conductance in dielectric materials.[35–38] Fig. 5b shows the TSC spectrum when the sample had been (black), and had not been illuminated (red) for 20 min at room temperature. The current peak around 100 °C in the TSC validates the thermal activation of the electrons from the gap states to the CB for the sample after light pre-illumination. Under the SBG light illumination, the photoinduced electrons will be firstly trapped at the gap states, which cannot be activated to the CB at low temperatures. As the temperature increases, the trapped electrons will be thermally activated to the CB states and contribute to the conductance peak. As a consequence, the combination of the *in situ* diffusion reflectance and photoconductances confirms that the SBG photons and heat can couple together to promote the VB electrons to the CB of the pristine TiO_2.

3.3. SBG light induced IPA dehydrogenation

The isopropanol molecule can be dehydrogenated by TiO_2 under light illumination; the process is dependent on the TiO_2 surface chemistry.[39] The lattice oxygens of TiO_2 surfaces were found to be unreactive with isopropanol in the absence of molecular O_2 under super-bandgap light illumination. Molecular O_2 must be involved in the reaction to donate oxygen atoms for taking hydrogens from the isopropanol molecule. It was also found that the reaction of molecular O_2 with isopropanol over TiO_2 surfaces cannot proceed in the absence of light. The isopropanol dehydrogenation should be initiated by electron–hole pair generation under UV light illumination and the subsequent trapping of one of them by surface species.[40] As O_2 is a good electron scavenger, one initial reaction is most likely to be $O_2 + e \rightarrow O_2^-$. Brinkley *et al.* studied the photocatalytic pathway of isopropanol dehydrogenation over a (110) rutile surface, and they attributed the photocatalytic reactivity to undissociated 2-propanol molecules coordinated at Ti^{4+} sites.[40] As the formed O_2^- is not a sufficiently strong base to abstract the hydrogens from the isopropanol

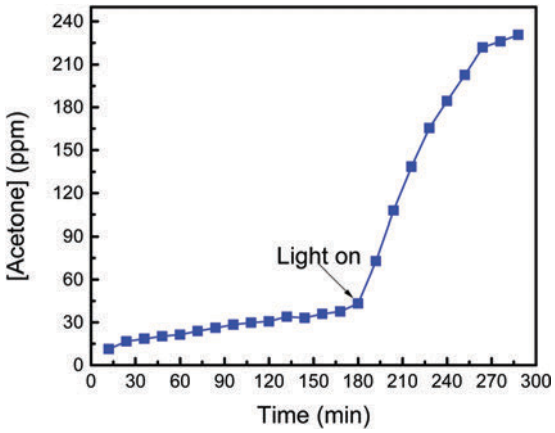

Fig. 6 Acetone evolution during the IPA catalytic conversion over the P25 TiO_2 in the dark and under the illumination of 500 nm monochromic light (light intensity: 35 mW cm ^{2}) at 100 °C.

molecule, the direct reaction between isopropanol and O_2^- is unlikely to occur. The trapping of a hole by isopropanol should greatly reduce the barrier to remove the hydrogen from the OH group and hydrogen bound to the tertiary carbon of isopropanol. Then, the dehydrogenation might occur through different pathways. The bridging oxygen of TiO_2 might be involved to abstract the hydrogens of the isopropanol molecule. It is also possible that the hydrogens can be abstracted by OH radicals formed from O_2^-.[40,41] It is considered that, although the detailed pathways of isopropanol dehydrogenation might be different, the initial steps should be hole trapping by undissociated isopropanol and electron trapping by molecular O_2. The above results show that the SBG light induced electrons can transfer to O_2, and the holes can also be captured by isopropanol molecules; this means that the isopropanol could also undergo dehydrogenation under SBG light illumination.

A 420 nm short wavelength cutting filter was used together with the 450 nm, 500 nm, 550 nm, and 600 nm band-passing filters to generate the different SBG monochromic lights from a Xe lamp and avoid leakage of UV light (Fig. S2, ESI†). It is seen that isopropanol can be dehydrogenated into acetone over the pristine TiO_2 under this SBG light illumination (Fig. S6, ESI†). Fig. 6 shows that acetone evolution in the dark is slow, but becomes much faster upon 500 nm light illumination. The light induced increase in the surface temperature is less than 2 °C (Fig. S7, ESI†) and it is also seen that the photocatalytic isopropanol dehydrogenation increases with light intensity (Fig. S8, ESI†); it is thus considered that the SBG light induced catalytic effect is not a photothermal effect. The photocatalytic activity is dependent on the light wavelength (Fig. S9, ESI†), which increases with photon energy. The photocatalytic effect also increases with temperature from 20 °C to 100 °C (Fig. S10, ESI†). Other by-products start to appear at high rates at 120 °C, resulting in a decrease in acetone yields. The by-products may be formed from an aldol condensation between acetone and isopropanol, which can result in mesityl oxides, like $(CH_3)_2C$ CHCOCH$_3$, 4-methyl-3-penten-2-one, or others.[40,42,43] In addition, it is also observed that formic acid and acetaldehyde can be formed as intermediates of the subsequent acetone PCO.[44] Therefore, the by-products can be produced from the reaction between the intermediate with isopropanol. GC-MS was used to identify the organic substances involved at 120 °C (Fig. S11, ESI†). In additional to isopropanol and acetone, isopropyl formate and formic acid were also seen during the sub-bandgap light induced reaction. Isopropyl formate is ascribed to the esterification reaction between the formic acid and isopropanol.

3.4. Effect of the light–heat synergism in the SBG photocatalytic response

Under illumination with monochromic SBG light, the acetone yields against E_g–$h\nu$ (photon energies of the 450, 500, 550, and 550 nm monochromic lights) are shown in Fig. 7a. The acetone yields are normalized based on photon number with wavelength; the 500 nm monochromic light is used as a reference. It is seen that the normalized acetone yields increase with E_g–$h\nu$ in an approximately exponential fashion; this result is in good accordance with the model where the exponential gap states are involved in the SBG light response. As shown in Fig. 7b, the

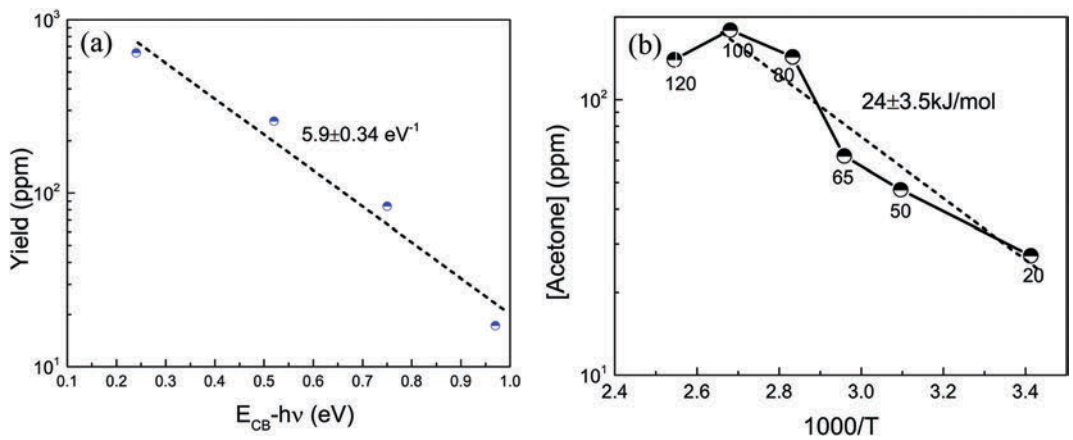

Fig. 7 (a) Dependence of the acetone yields after 140 min reaction on the difference between the TiO_2 bandgap (taken to be 3.0 eV) and the phonon energies ($h\nu$) of the SBG light; (b) dependence of the acetone yields after 84 min reaction on temperature in the Arrhenius mode.

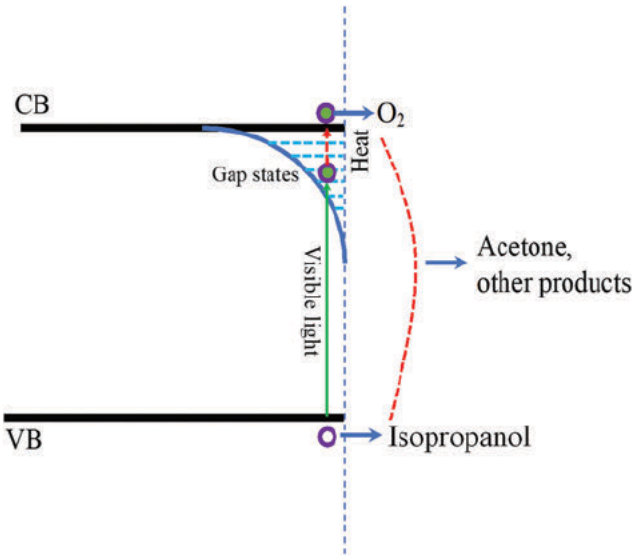

Fig. 8 Diagram of the proposed SBG light induced electron hole generation and the subsequent IPA to acetone photocatalytic conversion.

dependence of the acetone yield on temperatures shows that the SBG light induced isopropanol conversion is heat-assisted. The photocatalytic activity can increase 5 fold from 20 °C to 100 °C. Based on this data, the apparent activation energy (E_{app}) of the isopropanol-to-acetone conversion under 500 nm monochromic light illumination is estimated to be ~24 kJ mol^{-1}. Furthermore, the photocatalytic isopropanol dehydrogenation under double laser illumination was also performed (Fig. S12, ESI†). It is seen that the double lasers cannot induce a synergism for the photocatalytic properties as compared with the sum of the single laser induced effects. Therefore, the SBG responsive isopropanol photocatalysis does not involve a double photon synergism. Based on the above observations, the photocatalytic response is explained in Fig. 8. Under SBG light illumination, the VB electrons are firstly excited to the exponential band-gap tail-states, which are then thermally activated to the CB states. The CB electrons can then transfer to O_2 and the VB holes can transfer to isopropanol molecules, inducing dehydrogenation. Therefore, the light–heat synergism in the SBG light electronic transition contributes to the photocatalytic effect.

4. Conclusion

In summary, it was revealed from *in situ* diffusion reflectance and photoconductance that the VB electrons of pristine TiO_2 can be excited to the exponentially-distributed gap states, which are then thermally activated to the CB states. The SBG light response thus contains the SBG light–heat synergism. Isopropanol can be dehydrogenated into acetone by SBG illumination; the dependences of the photocatalytic activities on temperature and the SBG photon energy agree well with the light–heat synergism involving exponentially-distributed gap states. We gave a clear illustration of the mechanism with the SBG light response for pristine TiO_2 and its function for isopropanol photocatalysis. It is believed that our findings should be meaningful in understanding the physiochemical mechanism of SBG light induced photocatalysis in pristine materials, not limited to TiO_2.

Conflicts of interest

There are no conflicts of interest to declare.

Acknowledgements

B. L. thanks the National Natural Science Foundation of China (NSFC) (No. 51772230), the National Key Research and Development of China (No. 2017YFE0192600), and the 111 Project (No. B18038). B. Liu also thanks the Key R&D Project of Hubei Province, China (No. 2020BAB061). I. P. Parkin thanks the Wuhan University of Technology for a visiting professorship.

References

1 Q. Guo, C. Zhou, Z. Ma and X. Yang, Fundamentals of TiO_2 Photocatalysis: Concepts, Mechanisms, and Challenges, *Adv. Mater.*, 2019, **31**, 1901997.
2 K. Nakata and A. Fujishima, TiO_2 photocatalysis: Design and Applications, *J. Photochem. Photobiol., C*, 2012, **13**, 169–189.
3 X. Zhang, Y. L. Chen, R. S. Liu and D. P. Tsai, Plasmonic Photocatalysis, *Rep. Prog. Phys.*, 2013, **76**, 046401.
4 M. Schultz and T. P. Yoon, Solar Synthesis: Prospects in Visible Light Photocatalysis, *Science*, 2014, **343**, 1239176.
5 X. Lang, X. Chen and J. Zhao, Heterogeneous Visible Light Photocatalysis for Selective Organic Transformations, *Chem. Soc. Rev.*, 2014, **43**, 473–486.
6 J. Schneider, M. Matsuoka, M. Takeuchi, J. Zhang, Y. Horiuchi, M. Anpo and D. W. Bahnemann, Understanding TiO_2 Photocatalysis: Mechanisms and Materials, *Chem. Rev.*, 2014, **114**, 9919–9986.
7 Q. Guo, Z. Ma, C. Zhou, Z. Ren and X. Yang, Single Molecule Photocatalysis on TiO_2 Surfaces, *Chem. Rev.*, 2019, **119**, 11020–11041.
8 B. Liu, X. Zhao, C. Terashima, A. Fujishima and K. Nakata, Thermodynamic and Kinetic Analysis of Heterogeneous Photocatalysis for Semiconductor Systems, *Phys. Chem. Chem. Phys.*, 2014, **16**, 8751–8760.
9 H. Zhang and B. Liu, Preparation, Characterization, and Photocatalytic Properties of Self-Standing Pure and Cu-Doped TiO_2 Nanobelt Membranes, *ACS Omega*, 2021, **6**, 4534–4541.
10 B. Liu, J. Wang, I. P. Parkin and X. Zhao, The effect of Cu Dopants on Electron Transfer to O_2 and the Connection with Acetone Photocatalytic Oxidations over Nano-TiO_2, *Phys. Chem. Chem. Phys.*, 2021, **23**, 8300–8308.
11 K. Fouad, M. G. Alalm, M. Bassyouni and M. Y. Saleh, A Novel Photocatalytic Reactor for the Extended Reuse of

W–TiO_2 in the Degradation of Sulfamethazine, *Chemosphere*, 2020, **257**, 127270.
12 P. Salvador, Subbandgap Photoresponse of n-TiO2 Electrodes: Transient Photocurrent – Time Behavior, *Surf. Sci.*, 1987, **192**, 36–46.
13 M. A. Butler, M. Abramovich, F. Decker and J. F. Juliao, Subband Gap Response of TiO_2 and $SrTiO_3$ Photoelectrodes, *J. Electrochem. Soc.*, 1981, **128**, 200–204.
14 B. Liu, J. Yang, J. Wang, X. Zhao and K. Nakata, High Subband gap Response of TiO_2 Nanorod Arrays for Visible Photoelectrochemical Water Oxidations, *Appl. Surf. Sci.*, 2019, **465**, 192–200.
15 D. Vanmaekelbergh and L. Van Pieterson, Free Carrier Generation in Semiconductors Induced by Absorption of Subband-Gap Light, *Phys. Rev. Lett.*, 1998, **80**, 821–824.
16 Z. Wu, L. Li, X. Zhou, X. Zhao and B. Liu, Kinetics and Energetic Analysis of the Slow Dispersive Electron Transfer from Nano-TiO_2 to O_2 by In-situ Diffusion Reflectance and Laplace Transform, *Phys. Chem. Chem. Phys.*, 2021, **23**, 19901–19910.
17 B. Liu, H. Wu, X. Zhang, I. P. Parkin and X. Zhao, New Insight into the Role of Electron Transfer to O_2 in Photocatalytic Oxidations of Acetone over TiO_2 and the Effect of Au Cocatalyst, *J. Phys. Chem. C*, 2019, **123**, 30958–30971.
18 B. Liu, Z. Wu and L. Li, Kinetics Analysis of the Electron Transfer from Nano-TiO_2 to O_2 through on-line Absorptions and Theoretical Modeling, *J. Appl. Phys.*, 2021, **129**, 165106.
19 T. Yoshihara, R. Katoh, A. Furube, Y. Tamaki, M. Murai, K. Hara, S. Murata, H. Arakawa and M. Tachiya, Identification of Reactive Species in Photoexcited Nanocrystalline-TiO_2 Films by Wide-Wavelength-Range (400-2500 nm) Transient Absorption Spectroscopy, *J. Phys. Chem. B*, 2004, **108**, 3817–3823.
20 K. Yamanaka, T. Ohwaki and T. Morikawa, Charge-Carrier Dynamics in Cu- or Fe-Loaded Nitrogen-Doped TiO_2 Powder Studied by Femtosecond Diffuse Reflectance Spectroscopy, *J. Phys. Chem. C*, 2013, **117**, 16448–16456.
21 K. Sakaguchi, K. Shimakawa and K. Hatanaka, Dynamic Responses of Photoconduction in TiOx Films Prepared by Radio Frequency Magnetron Sputtering, *Jpn. J. Appl. Phys.*, 2010, **49**, 091103.
22 K. Sakaguchi, K. Shimakawa and Y. Hatanaka, Photoconductive Characteristics of Hydro-Oxygenated Amorphous Titanium Oxide Films Prepared by Remote Plasma-Enhanced Chemical Vapor Deposition, *Jpn. J. Appl. Phys.*, 2006, **45**, 4183–4186.
23 X. Mao, X. Lang, Z. Wang, Q. Hao, B. Wen, Z. Ren, D. Dai, C. Zhou, L. M. Liu and X. Yang, Band-Gap States of TiO_2(110): Major Contribution from Surface Defects, *J. Phys. Chem. Lett.*, 2013, **4**, 3839–3844.
24 J. F. Li, R. Lazzari, S. Chenot and J. Jupille, Contributions of Oxygen Vacancies and Titanium Interstitials to Band-gap States of Reduced Titania, *Phys. Rev. B*, 2018, **97**, 041403.
25 B. Liu, X. Zhao, J. Yu, I. P. Parkin, A. Fujishima and K. Nakata, Intrinsic Intermediate Gap States of TiO_2 Materials and Their Roles in Charge Carrier Kinetics, *J. Photochem. Photobiol., C*, 2019, **39**, 1–57.
26 K. Yamanaka and T. Morikawa, Charge-Carrier Dynamics in Nitrogen-Doped TiO_2 Powder Studied by Femtosecond Time-Resolved Diffuse Reflectance Spectroscopy, *J. Phys. Chem. C*, 2012, **116**, 1286–1292.
27 S. Shen, X. Wang, T. Chen, Z. Feng and C. Li, Transfer of Photoinduced Electrons in Anatase–Rutile TiO_2 Determined by Time-Resolved Mid-Infrared Spectroscopy, *J. Phys. Chem. C*, 2014, **118**, 12661–12668.
28 A. Yamakata, T. Ishibashi and H. Onishi, Water- and Oxygen-Induced Decay Kinetics of Photogenerated Electrons in TiO_2 and Pt/TiO_2: A Time-Resolved Infrared Absorption Study, *J. Phys. Chem. B*, 2001, **105**, 7258–7262.
29 B. Liu, L. Li, Z. Wu, X. Zhou and X. Zhao, Exponential and Gaussian Traps in Nano-TiO_2 and their Function in Kinetics of the Electron Transfer to O_2, *J. Appl. Phys.*, 2021, **130**, 035102.
30 A. Petrozza, C. Groves and H. J. Snaith, Electron Transport and Recombination in Dye-Sensitized Mesoporous TiO_2 Probed by Photoinduced Charge-Conductivity Modulation Spectroscopy with Monte Carlo Modeling, *J. Am. Chem. Soc.*, 2008, **130**, 12912–12920.
31 J. Nelson, S. A. Haque, D. R. Klug and J. R. Durrant, Trap-limited Recombination in Dye-Sensitized Nanocrystalline Metal Oxide Electrodes, *Phys. Rev. B: Condens. Matter Mater. Phys.*, 2001, **63**, 205321.
32 G. Adriaenssens, S. Baranovskii, W. Fuhs, J. Jansen and Ö. Öktu, Photoconductivity Response Time in Amorphous Semiconductors, *Phys. Rev. B: Condens. Matter Mater. Phys.*, 1995, **51**, 9661–9667.
33 J. A. Navio, G. Coldn. and J. M. Herrmann, Photoconductive and photocatalytic properties of $ZrTiO_4$. Comparison with the parent oxides TiO_2 and ZrO_2, *J. Photochem. Photobiol., A*, 1997, **108**, 179–185.
34 B. Liu, H. Wu and I. P. Parkin, Gaseous Photocatalytic Oxidation of Formic Acid over TiO_2: A Comparison between the Charge Carrier Transfer and Light-Assisted Mars–van Krevelen Pathways, *J. Phys. Chem. C*, 2019, **123**, 22261–22272.
35 *Thermally Stimulated Relaxation in Solids*, ed. P. Bräunlich, Springer-Verlag, Berlin, 1979.
36 R. H. Bube and S. M. Thomsen, Photoconductivity and Crystal Imperfections in Cadmium Sulfide Crystals. Part I. Effect of Impurities, *J. Chem. Phys.*, 1955, **23**, 15–17.
37 R. H. Bube and S. M. Thomsen, Photoconductivity and crystal imperfections in cadmium sulfide crystals. Part II. Determination of characteristic photoconductivity quantities, *J. Chem. Phys.*, 1955, **23**, 18–25.
38 A. Bhatnagar, Y. H. Kim, D. Hesse and M. Alexe, Persistent Photoconductivity in Strained Epitaxial $BiFeO_3$ Thin Films, *Nano Lett.*, 2014, **14**, 5224–5228.
39 O. Bondarchuk, Y. K. Kim, J. M. White, J. Kim, B. D. Kay and Z. Dohnalek, Surface Chemistry of 2-Propanol on TiO_2(110): Low- and High-Temperature Dehydration, Isotope Effects, and Influence of Local Surface Structure, *J. Phys. Chem. C*, 2007, **111**, 11059–11067.

40 D. Brinkley and T. Engel, Photocatalytic Dehydrogenation of 2-Propanol on TiO_2(110), *J. Phys. Chem. B*, 1998, **102**, 7596–7605.
41 B. H. J. Bielski, D. E. Cabelli and R. L. Arudi, Reactivity of HO_2/O_2^- Radicals in Aqueous Solution, *J. Phys. Chem. Ref. Data*, 1985, **14**, 1041–1052.
42 W. Xu and D. Raftery, Photocatalytic Oxidation of 2-Propanol on TiO_2 Powder and TiO_2 Monolayer Catalysts Studied by Solid-State NMR, *J. Phys. Chem. B*, 2001, **105**, 4343–4349.
43 M. El-Maazawi, A. N. Finken, A. B. Nair and V. H. Grassian, Adsorption and Photocatalytic Oxidation of Acetone on TiO_2: An *in situ* Transmission FT-IR Study, *J. Catal.*, 2000, **191**, 138–146.
44 R. I. Bickley and R. K. M. Jayanty, Photo-adsorption and photo-catalysis on titanium dioxide surfaces. Photo-adsorption of oxygen and the photocatalyzed oxidation of isopropanol, *Faraday Discuss. Chem. Soc.*, 1974, **58**, 194.